Contribution from the Department of Chemistry, Monash University, Clayton, Victoria 3168, Australia, and Department of Physical and Inorganic Chemistry, University of Adelaide, Adelaide, South Australia 5001, Australia

Structural and Electronic Properties of Six-Coordinate Mixed Aquo(imidazole)iron(III) Schiff-Base Complexes. Crystal Structure of [Fe(3-MeO-salen)(5-Ph-imd)(H_2O)]BPh_4

BRENDAN J. KENNEDY,[†] GAVIN BRAIN,[†] ERNST HORN,[‡] KEITH S. MURRAY,[*†] and MICHAEL R. SNOW[‡]

Received June 18, 1984

The first structurally characterized mixed aquo–imidazole axially ligated iron(III) chelate complexes are described. These cationic complexes contain a tetradentate Schiff-base ligand such as *N,N'*-ethylenebis(3-methoxysalicylaldimine) (i.e., 3-MeO-salen^{2-}) in the equatorial plane and have a tetraphenylborate counterion. Reasons are given for the preferred crystallization of the 1:1 Fe:imidazole adduct rather than the 1:2 adduct. A crystal structure determination of one example, [Fe(3-MeO-salen)(5-Ph-imd)(H_2O)]$BPh_4 \cdot H_2O$, shows that the iron atom is in the plane of the N_2O_2 donor set with axial distances of Fe–OH_2 = 2.205 Å and Fe–N(imd) = 2.132 Å. The compound ($C_{51}H_{48}BFeN_4O_5$) crystallizes in the triclinic space group $P\bar{1}$ with a = 13.290 (3) Å, b = 14.536 (4) Å, c = 14.673 (3) Å, α = 68.00 (2)°, β = 58.64 (2)°, γ = 69.54 (2)°, and Z = 2. The cationic complex molecules are held together as weakly bridged dimeric units via hydrogen bonding between the axial water and the phenoxo oxygen and methoxo oxygen of the Schiff base in the neighboring molecule. This interaction is detected in low-temperature susceptibility studies that display evidence for weak antiferromagnetic exchange interactions between the high-spin $^6A_1$ iron(III) centers. A combination of variable-temperature susceptibilities and Mössbauer effect and ESR spectroscopies has yielded values of the zero-field splitting parameter in these compounds. Finally, a brief comparison of the electronic and structural features of the present compounds is made with those of iron(III) hemes such as sperm whale metaquomyoglobin, which also possess aquo–imidazole ligation. Synthetic iron(III) porphyrins of this type are not yet known.

Introduction

Six-coordinate bis-ligated iron(III) porphyrin and Schiff-base complexes of general types [Fe(tetradentate)$(L)_2$]Y (L = imidazole or pyridine base; Y = ClO_4^-, BF_4^-, BPh_4^-, etc.) display an interesting range of structural and electronic effects.[1-9] Variations of in-plane chelate, axial base, and counteranion can lead to high-spin ($S = {}^5/_2$) or low-spin ($S = {}^1/_2$) states on Fe(III) and also to spin-crossover behavior. We,[9,10] and others,[1-8] have been investigating such behavior in both the porphyrin and salen-like systems in an attempt to systematically delineate the important factors that lead to crossover behavior. The recent structural work of Scheidt et al.[4] on the octaethylporphyrin system [Fe(OEP)(3-Cl-py)$_2$]ClO_4, first studied by Hill et al.[2], has also demonstrated unusual solid-state effects as well as the crystallization of multiple phases, each with different magnetic properties. Somewhat related effects in a series of bis(tridentate Schiff base) complexes have been observed by Hendrickson et al.[11] although fewer crystal structures[12] were available compared to the OEP series. Solution and thermodynamic studies on the formation of Lewis-base adducts of these types by optical, NMR, and ESR methods have generally shown the pronounced stability of the 1:2 adduct compared to the 1:1 intermediate. In the porphyrin series this invariably leads to isolation of the bis adduct with very little evidence for a finite existence of the mono adduct.[13,14] The Schiff-base compounds seem to behave in a similar manner although we have found that, for certain combinations of base and counterion, it is possible to crystallize the 1:1 adduct. In this paper we describe the crystal structure of one such compound, [Fe(3-MeO-salen)(5-Ph-imd)(H_2O)]BPh_4 (3), in which the sixth coordination site is occupied by a water molecule. The electronic properties of this and three related high-spin compounds have been investigated by means of magnetic, ESR, and Mössbauer spectral measurements. From the bioinorganic point of view, this mixed aquo–imidazole coordination of Fe(III) provides a useful structural and electronic model for the similarly coordinated Fe(III) sites found in metaquomyoglobin.[15] While some mixed adducts of Fe(III) porphyrins have recently been structurally characterized,[16] there are no examples to our knowledge of aquo–imidazole derivatives.

Experimental Section

Synthesis. [Fe(3-MeO-salen)(pyz)(H_2O)]$BPh_4 \cdot H_2O$ (1). A 0.5-g portion of Fe(3-MeO-salen)Cl·H_2O[9,17] was suspended in 40 mL of absolute methanol and 0.5 g of pyrazole added. The solution was then refluxed for 10 min and filtered, while hot, into a freshly prepared methanol solution (10 mL) of $NaBPh_4$ (0.4 g). Evaporation of the solvent from the resulting solution resulted in the formation of fine black needles. These were filtered, washed twice with 5-mL portions of *ice-cold*

Table I. Microanalytical Data and Room-Temperature Magnetic Moments of [Fe(3-R-salen)(L)(H_2O)]$BPh_4 \cdot nH_2O$

complex	R	L	n	% anal. (% calcd) C	H	N	μ_{eff}(295 K), μ_B
1	MeO	pyz	1	67.75 (67.86)	5.67 (5.69)	7.31 (7.03)	5.91
2	EtO	pyz	0.5	68.14 (67.72)	6.05 (6.05)	6.32 (6.72)	5.80
3	MeO	5-Ph-imd	1	69.46 (69.48)	5.48 (5.71)	5.98 (6.35)	5.77
4	EtO	5-Ph-imd	0.5	70.52 (70.68)	6.43 (5.93)	6.35 (6.22)	5.63

[†] Monash University.
[‡] University of Adelaide.

(1) Scheidt, W. R.; Reed, C. A. *Chem. Rev. A.* **1981**, *81*, 543.
(2) Hill, H. A. O.; Skyte, P. D.; Buchler, J. W.; Leuken, H.; Tonn, M.; Gregson, A. K.; Pellizer, G. J. *J. Chem. Soc., Chem. Commun.* **1979**, 151.
(3) Gregson, A. K. *Inorg. Chem.* **1981**, *20*, 81.
(4) Scheidt, W. R.; Geiger, D. K.; Hayes, R. G.; Lang, G. *J. Am. Chem. Soc.* **1983**, *105*, 2625 and references therein.
(5) Scheidt, W. R.; Cohen, I. A.; Kastner, M. E. *Biochemistry* **1979**, *18*, 3546.
(6) Collman, J. P.; Sorell, T.N.; Hodgson, K. G.; Kulshrestha, A. K.; Strouse, C. E. *J. Am. Chem. Soc.* **1977**, *99*, 5180.
(7) (a) Ohshio, H.; Maeda, V.; Takashima, Y. *Inorg. Chem.* **1983**, *22*, 2684. (b) Maeda, Y.; Ohshio, H.; Takashima, Y. *Chem. Lett.* **1982**, 943.
(8) (a) Nishida, Y.; Oshio, S.; Kida, S. *Bull. Chem. Soc. Jpn.* **1977**, *50*, 119. (b) Nishida, Y.; Oshio, S.; Kida, S. *Chem. Lett.* **1975**, 79.
(9) Kennedy, B. J.; Murray, K. S., to be submitted for publication.
(10) Kennedy, B. J.; Fallon, G. D.; Gatehouse, B. M. K. C.; Murray, K. S. *Inorg. Chem.* **1984**, *23*, 580.
(11) (a) Haddad, M. S.; Lynch, M. W.; Federer, W. D.; Hendrickson, D. N. *Inorg. Chem.* **1981**, *20*, 123. (b) Haddad, M. S.; Federer, W. D.; Lynch, M. W.; Hendrickson, D. N. *Inorg. Chem.* **1981**, *20*, 131.
(12) Summerton, A. P.; Diamantis, A. A.; Snow, M. R. *Inorg. Chim. Acta* **1978**, *27*, 123.
(13) Walker, F. A.; Lo, M. W.; Ree, M. T. *J. Am. Chem. Soc.* **1976**, *98*, 5552.
(14) (a) La Mar, G. N.; Walker, R. A. *J. Am. Chem. Soc.* **1972**, *94*, 8607. (b) Saterlee, J. D.; La Mar, G. N.; Frye, J. S. *J. Am. Chem. Soc.* **1976**, *98*, 7275.
(15) (a) Takano, T. *J. Mol. Biol.* **1977**, *110*, 537. (b) Ladner, R. C.; Heidner, F. J.; Perutz, M. F. *J. Mol. Biol.* **1977**, *114*, 385.
(16) (a) Scheidt, W. R.; Lee, Y. J.; Luangdilov, W.; Haller, K.; Anzai, K.; Hatano, K. *Inorg. Chem.* **1983**, *22*, 1516. (b) Adams, K. M.; Rasmussen, P. G.; Scheidt, W. R.; Hatano, K. *Inorg. Chem.* **1979**, *18*, 1892. (c) Scheidt, W. R.; Lee, Y. T.; Geiger, D. K.; Taylor, K.; Hatano, K. *J. Am. Chem. Soc.* **1982**, *104*, 3367.
(17) Gullotti, M.; Casella, L.; Pasini, A.; Ugo, R. *J. Chem. Soc., Dalton Trans.* **1977**, 339.

0020-1669/85/1324-1647$01.50/0

Table II. Non-Hydrogen Atom Coordinates for [Fe(3-MeO-salen)(5-Ph-imd)(H_2O)]BPh_4[a]

atom	x	y	z	atom[b]	x	y	z
Fe(1)	37837 (9)	12754 (7)	9604 (9)	C(22)	5701 (4)	−1587 (3)	3513 (4)
O(1)	5560 (4)	1179 (3)	−475 (4)	C(23)	5129 (4)	−1265 (3)	2845 (4)
O(2)	3172 (4)	866 (3)	304 (4)	C(24)	4877 (4)	−239 (3)	2367 (4)
O(3)	2292 (5)	−161 (4)	−88 (4)	C(25)	5195 (4)	463 (3)	2557 (4)
O(4)	4344 (4)	8 (3)	1722 (4)	C(26)	4794 (8)	−2904 (6)	3214 (6)
O(5)	4770 (5)	−1882 (3)	2608 (4)	C(27)	4945 (6)	1545 (5)	2130 (6)
N(1)	2066 (5)	1466 (4)	2331 (5)	C(28)	4762 (4)	2944 (2)	3704 (4)
N(2)	133 (6)	1434 (5)	3441 (6)	C(29)	3533 (4)	3205 (2)	4022 (4)
N(3)	3489 (5)	2755 (4)	75 (5)	C(30)	3025 (4)	4182 (2)	3617 (4)
N(4)	4392 (5)	1990 (4)	1499 (5)	C(31)	3747 (4)	4897 (2)	2894 (4)
C(1)	1063 (8)	1325 (6)	2425 (7)	C(32)	4977 (4)	4636 (2)	2576 (4)
C(2)	542 (7)	1677 (5)	3986 (7)	C(33)	5484 (4)	3659 (2)	2981 (4)
C(3)	1724 (7)	1700 (6)	3309 (8)	C(34)	6569 (3)	4587 (3)	3766 (4)
C(4)	24 (5)	2497 (4)	5431 (5)	C(35)	6944 (3)	4995 (3)	4233 (4)
C(5)	−668 (5)	2628 (4)	6499 (5)	C(36)	8153 (3)	4783 (3)	3987 (4)
C(6)	−1612 (5)	2115 (4)	7241 (5)	C(37)	8986 (3)	4163 (3)	3273 (4)
C(7)	−1864 (5)	1471 (4)	6914 (5)	C(38)	8610 (3)	3755 (3)	2806 (4)
C(8)	−1172 (5)	1341 (4)	5846 (5)	C(39)	7402 (3)	3967 (3)	3053 (4)
C(9)	−228 (5)	1854 (4)	5105 (5)	C(40)	7125 (4)	1669 (3)	3986 (3)
C(10)	2939 (7)	3085 (6)	−512 (7)	C(41)	7565 (4)	646 (3)	4321 (3)
C(11)	1776 (5)	2951 (3)	−1301 (5)	C(42)	8442 (4)	103 (3)	3540 (3)
C(12)	1287 (5)	2406 (3)	−1526 (5)	C(43)	8879 (4)	582 (3)	2426 (3)
C(13)	1434 (5)	1359 (3)	−1132 (5)	C(44)	8438 (4)	1605 (3)	2091 (3)
C(14)	2069 (5)	858 (3)	−514 (5)	C(45)	7561 (4)	2149 (3)	2872 (3)
C(15)	2557 (5)	1404 (3)	−289 (5)	C(46)	7163 (4)	3506 (3)	603 (4)
C(16)	2411 (5)	2450 (3)	−683 (5)	C(47)	7595 (4)	3827 (3)	−534 (4)
C(17)	1860 (8)	−774 (6)	−317 (8)	C(48)	8457 (4)	4433 (3)	−1151 (4)
C(18)	4071 (7)	3437 (6)	94 (7)	C(49)	8888 (4)	4718 (3)	−631 (4)
C(19)	4077 (8)	3112 (6)	1181 (7)	C(50)	8456 (4)	4397 (3)	506 (4)
C(20)	5767 (4)	141 (3)	3225 (4)	C(51)	7594 (4)	3791 (3)	1123 (4)
C(21)	6020 (4)	−885 (3)	3703 (4)	B(1)	6997 (8)	3405 (6)	2517 (8)

[a] Fe coordinates ×100 000; other atom coordinates ×10 000. [b] Carbons C(28) to C(51) are disposed around B(1) in the BPh_4 group.

methanol, and then air-dried, yield 65–75%.

If the reaction mixture was allowed to stand for periods longer than ca. 3 h, then the product was often comtainated by red-orange crystals identified by IR and magnetic susceptibility measurements as [Fe(3-MeO-salen)]$_2$O.

[Fe(3-MeO-salen)(5-Ph-imd)(H_2O)]BPh_4·H_2O (3). This compound was prepared in the same manner to that described above. Crystals suitable for the X-ray diffraction study were obtained by allowing the solution to evaporate overnight. Although this resulted in appreciable amounts of the μ-oxo dimer being formed, small black crystals of the product were also obtained. The identity of these crystals was confirmed by microanalysis (Table I) and by comparison of the Mössbauer spectra with that of an authentic sample.

[Fe(3-EtO-salen)(L)(H_2O)]BPh_4·0.5H_2O (L = pyz (2), Ph-imd (4)). These were prepared in a manner analogous tc that described above except that Fe(EtO-salen)Cl·H_2O was used.

Crystal Data. An orange prismatic crystal of dimensions 0.23 × 0.28 × 0.31 mm^3 was mounted on a glass fiber and coated with cyanoacrylate "super glue". The lattice parameters at 25 °C were determined by a least-squares fit to the setting angles of 25 independent reflections, measured and refined by scans performed on an Enraf-Nonius CAD-4 four-circle diffractometer employing monochromated Mo Kα radiation. Crystal data for $C_{51}H_{48}BFeN_4O_5$: formula wt 862.59, triclinic space group $P\bar{1}$, a = 13.290 (3) Å, b = 14.536 (4) Å, c = 14.673 (3) Å, α = 68.00 (2)°, β = 58.64 (2)°, γ = 69.54 (2)°; V = 2200.9 Å^3, D_{calcd} = 1.302 g cm^{-3}, Z = 2; μ(Mo K$_\alpha$) = 3.91 cm^{-1}; λ(Mo K$_\alpha$) = 0.7107 Å; F(000) = 904 electrons.

Intensity data ($\pm h$, $\pm kl$), were collected in the range $1.5 < \theta < 20°$ with an $\omega-(n/3)\theta$ scan, where $n(=3)$ was optimized by profile analysis of several reflections. The ω-scan angle and horizontal counter apertures employed were (1.23 + 0.35 tan θ)° and (2.4 + 0.5 tan θ) mm, respectively. Three standard reflections, monitored after every 1 h of data collection, indicated that by completion of the data collection no decomposition had occurred. Data reduction and application of Lorentz and polarization corrections were performed by using program SUSCAD.[18] Absorption corrections were applied with program ABSORB.[18] Maximum and minimum transmission factors were estimated to be 0.98 and 0.91, respectively. Of the 3364 reflections collected, 570 with $I < 2.5\sigma(I)$ were considered unobserved and not used in the calculations. The internal consistency index ($R\pm$) calculated after merging equivalent reflections was 0.0042.

Solutions and Refinement. The structure was solved and refined by using the heavy-atom technique with the program SHELX.[18] Successive difference synthesis located all non-hydrogen atoms of the structure. During the least-squares refinements the program minimized the function $\sum w(\Delta F)^2$. In the blocked-matrix least-squares refinements the hydrogen positions were initially calculated (C–H = 0.97, 1.08 (benzene)) and then allowed to ride in fixed orientation to the respective carbon atoms. The atoms in the methyl groups and benzene rings were refined as rigid groups with all ring carbon atoms constrained to regular hexagons (C–C = 1.395 Å). A weighting scheme was applied and refined, converging at $w = 7.9/(\sigma^2(F_o) + 0.000\,136(F_o)^2)$. The refinement converged with R = 0.064 and R_w = 0.075 at which stage the largest peak in the final difference map was less than 0.6 e Å^{-3}. All scattering factors and anomalous terms were taken from the International Tables (Vol. IV). The final positional parameters are listed in Table II. Bond lengths and angles are given in Tables III and IV, respectively. The thermal parameters, hydrogen parameters, and observed and calculated structure factors are available as supplementary material.

Table III. Bond Lengths (Å) for [Fe(3-MeO-salen)(5-Ph-imd)(H_2O)]BPh_4

O(1)–Fe(1)	2.205 (4)	O(2)–Fe(1)	1.880 (7)
O(4)–Fe(1)	1.891 (4)	N(1)–Fe(1)	2.132 (5)
N(3)–Fe(1)	2.082 (5)	N(4)–Fe(1)	2.060 (9)
C(15)–O(2)	1.353 (9)	C(14)–O(3)	1.369 (6)
C(17)–O(3)	1.424 (16)	C(24)–O(4)	1.341 (10)
C(23)–O(5)	1.367 (10)	C(26)–O(5)	1.419 (9)
C(1)–N(1)	1.351 (15)	C(3)–N(1)	1.402 (14)
C(1)–N(2)	1.381 (10)	C(2)–N(2)	1.366 (17)
C(10)–N(3)	1.269 (15)	C(18)–N(3)	1.473 (15)
C(19)–N(4)	1.489 (9)	C(27)–N(4)	1.323 (12)
C(3)–C(2)	1.360 (11)	C(9)–C(2)	1.483 (11)
C(16)–C(10)	1.492 (15)	C(19)–C(18)	1.491 (16)
C(27)–C(25)	1.448 (8)		

Physical Methods. Magnetic susceptibilities of polycrystalline samples were measured at 10 kG on an Oxford Instrument Faraday balance.[19] Samples were carefully checked for any anomalous field dependence at both 4.2 and 300 K, and none were found to be present. ESR spectra

(18) Guss, J. M. "SUSCAD, Program for Data Reduction"; 1979. Guss, J. M. "ABSORB, Program for Absorption Corrections"; 1980. Sheldrick, G. M. "SHELX, Single Crystal Refinement Program"; 1976.

(19) Mackay, D. J.; Evans, S. V.; Martin, R. L. *J. Chem. Soc., Dalton Trans.* **1976**, 1515.

Table IV. Bond Angles (deg) for $[Fe(3\text{-MeO-salen})(5\text{-Ph-imd})(H_2O)]BPh_4$

O(2)-Fe(1)-O(1)	90.4 (2)	O(4)-Fe(1)-O(1)	89.2 (2)
O(4)-Fe(1)-O(2)	100.5 (2)	N(1)-Fe(1)-O(1)	176.3 (2)
N(1)-Fe(1)-O(2)	91.5 (3)	N(1)-Fe(1)-O(4)	93.5 (2)
N(3)-Fe(1)-O(1)	83.6 (2)	N(3)-Fe(1)-O(2)	89.7 (3)
N(3)-Fe(1)-O(4)	167.6 (3)	N(3)-Fe(1)-N(1)	93.3 (2)
N(4)-Fe(1)-O(1)	88.2 (2)	N(4)-Fe(1)-O(2)	169.2 (2)
N(4)-Fe(1)-O(4)	90.2 (3)	N(4)-Fe(1)-N(1)	89.3 (3)
N(4)-Fe(1)-N(3)	79.5 (3)	C(15)-O(2)-Fe(1)	131.4 (4)
C(17)-O(3)-C(14)	117.1 (7)	C(24)-O(4)-Fe(1)	131.4 (4)
C(26)-O(5)-C(23)	118.2 (8)	C(1)-N(1)-Fe(1)	123.9 (7)
C(3)-N(1)-Fe(1)	130.3 (6)	C(3)-N(1)-C(1)	105.8 (7)
C(2)-N(2)-C(1)	108.8 (8)	C(10)-N(3)-Fe(1)	126.4 (7)
C(18)-N(3)-Fe(1)	114.2 (6)	C(18)-N(3)-C(10)	119.2 (7)
C(19)-N(4)-Fe(1)	113.7 (7)	C(27)-N(4)-Fe(1)	126.1 (5)
N(2)-C(1)-N(1)	109.0 (10)	C(3)-C(2)-N(2)	106.4 (9)
C(9)-C(2)-N(2)	123.1 (7)	C(9)-C(2)-C(3)	130.5 (11)
C(2)-C(3)-N(1)	110.0 (11)	C(8)-C(9)-C(2)	119.9 (8)
C(16)-C(10)-N(3)	124.5 (7)	C(13)-C(14)-O(3)	126.3 (7)
C(15)-C(14)-O(3)	113.7 (6)	C(14)-C(15)-O(2)	116.7 (4)
C(16)-C(15)-O(2)	123.3 (7)	C(11)-C(16)-C(10)	116.6 (5)
C(15)-C(16)-C(10)	123.3 (7)	C(19)-C(18)-N(3)	108.3 (7)
C(18)-C(19)-N(4)	109.5 (9)	C(22)-C(23)-O(5)	125.1 (4)
C(24)-C(23)-O(5)	114.9 (6)	C(23)-C(24)-O(4)	116.4 (6)
C(25)-C(24)-O(4)	123.6 (4)	C(27)-C(25)-C(20)	115.3 (7)
C(27)-C(25)-C(24)	124.6 (7)	C(25)-C(27)-N(4)	123.9 (9)
B(1)-C(33)-C(28)	123.5 (4)	B(1)-C(33)-C(32)	116.5 (4)
B(1)-C(39)-C(34)	122.3 (4)	B(1)-C(39)-C(38)	117.7 (5)
B(1)-C(45)-C(40)	117.7 (4)	B(1)-C(45)-C(44)	122.3 (4)
B(1)-C(51)-C(46)	117.6 (6)	B(1)-C(51)-C(50)	122.3 (7)
C(39)-B(1)-C(33)	111.9 (6)	C(45)-B(1)-C(33)	112.8 (6)
C(45)-B(1)-C(39)	105.0 (7)	C(51)-B(1)-C(33)	105.9 (7)
C(51)-B(1)-C(39)	112.7 (6)	C(51)-B(1)-C(45)	108.7 (5)

were recorded on a Varian E-12 X-band spectrometer.

Mössbauer spectra were measured as described elsewhere.[20] All the spectra were fitted to Lorentzian line shapes, and the velocity and isomer shifts are relative to iron metal at room temperature.

Results and Discussion

Formation of Mono(base) Complexes $[Fe(3\text{-R-salen})(L)(H_2O)]^+X^-$. During attempts[9] to prepared some six-coordinate Lewis base adducts of Fe^{III}(3-MeO-salen) and Fe^{III}(3-EtO-salen) using either pyrazole or 4(5)-phenylimidazole, the crystalline products were often contaminated with large amounts of the corresponding μ-oxo dimer. This was especially so if the reaction solutions were allowed to stand for long periods. In attempts to overcome this problem it was decided to rapidly isolate the adducts from solution by evaporating off the majority of the solvent following the addition of $NaBPh_4$. Surprisingly, the analytical data on these complexes indicated that only one Lewis base was present together with variable amounts of solvated water. Under identical reaction conditions both imidazole and *N*-methylimidazole did, however, yield the bis(base) adducts $[Fe(3\text{-R-salen})(L)_2]BPh_4$. Similarly, when pyrazole or 4-phenylimidazole was reacted with Fe(salen)Cl the bis adducts were obtained.[9]

The ESR spectrum of the reaction mixture containing $Fe(3\text{-EtO-salen})Cl\cdot H_2O$, 4-Ph-imd, and $NaBPh_4$ measured at 77 K (Figure 1) showed two main sets of signals, the first at $g = 4.46$, typical of high-spin Fe(III), and the second typical of low-spin Fe(III) with g values of 2.32, 2.12, and 1.90. The low-spin signals are thought to be due to bis(base) adduct being present in solution, while the high-spin signal is due to the mono(base) adduct and/or starting material. The relative intensities of the two signals indicate that, in solution, the bis adduct is the major species present. The solution behavior may be explained in terms of the following equilibria:

$$[Fe(SB)]^+ \overset{L}{\rightleftharpoons} [Fe(SB)L]^+ \overset{L}{\rightleftharpoons} [Fe(SB)L_2]^+$$

where SB is a tetradentate Schiff base.

(20) Mitchell, A. J.; Murray, K. S.; Newman, P. J.; Clark, P. E. *Aust. J. Chem.* **1977**, *30*, 2439.

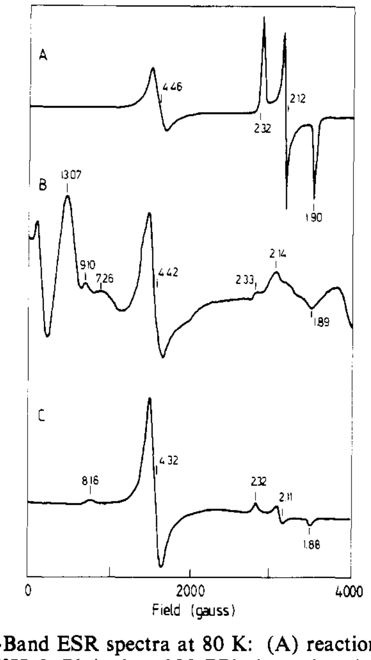

Figure 1. X-Band ESR spectra at 80 K: (A) reaction mixture $[Fe(3\text{-EtO-salen})Cl]H_2O$, Ph-imd, and $NaBPh_4$ in methanol; (B) powder sample; (C) solid redissolved in methanol.

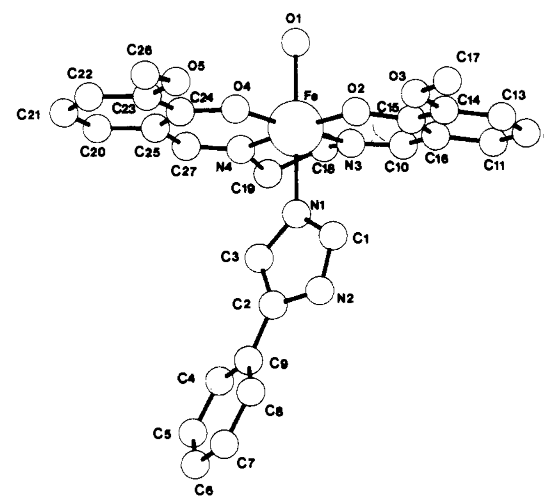

Figure 2. Structure of $[Fe(3\text{-MeO-salen})(5\text{-Ph-imd})(H_2O)]^+$ showing the numbering scheme of the atoms.

The presence of a large excess of L favors the formation of the bis adduct. Such equilibria have been extensively studied for Fe(III) porphyrin complexes,[13,1] and generally it is found that the formation of the bis adduct is strongly favored. The presence of a relatively strong high-spin signal in the present case indicates that while the low-spin bis adduct is also formed, its stability may not be very much greater than that of the mono adduct. Despite the fact that the bis adduct is the major species in solution for certain combinations of R, L, and X, it is the mono(base) adduct that crystallizes out of solution, suggesting that in these cases its solubility is less than that of the corresponding bis adduct.

The ready formation of the μ-oxo dimer in the present system can probably be attributed to the hydrolysis of the mono adduct, $[Fe(SB)(L)(H_2O)]^+$ with subsequent dissociation of the Lewis base, L.

Crystal and Molecular Structure of $[Fe(3\text{-MeO-Salen})(5\text{-Ph-imd})(H_2O)]BPh_4$ (3). Figure 2 shows the molecular structure of $[Fe(3\text{-MeO-salen})(5\text{-Ph-imd})(H_2O)]^+$ and the atomic numbering scheme employed for all non-hydrogen atoms of the molecule. The coordination sphere about the iron atom has a distorted octahedral geometry. The large deviation from 90° of the equatorial angles N3–Fe–N4 = 79.5 (3)° and O2–Fe–O4 = 100.5 (2)° are determined by the methoxysalicylaldimine ligand and are usual for

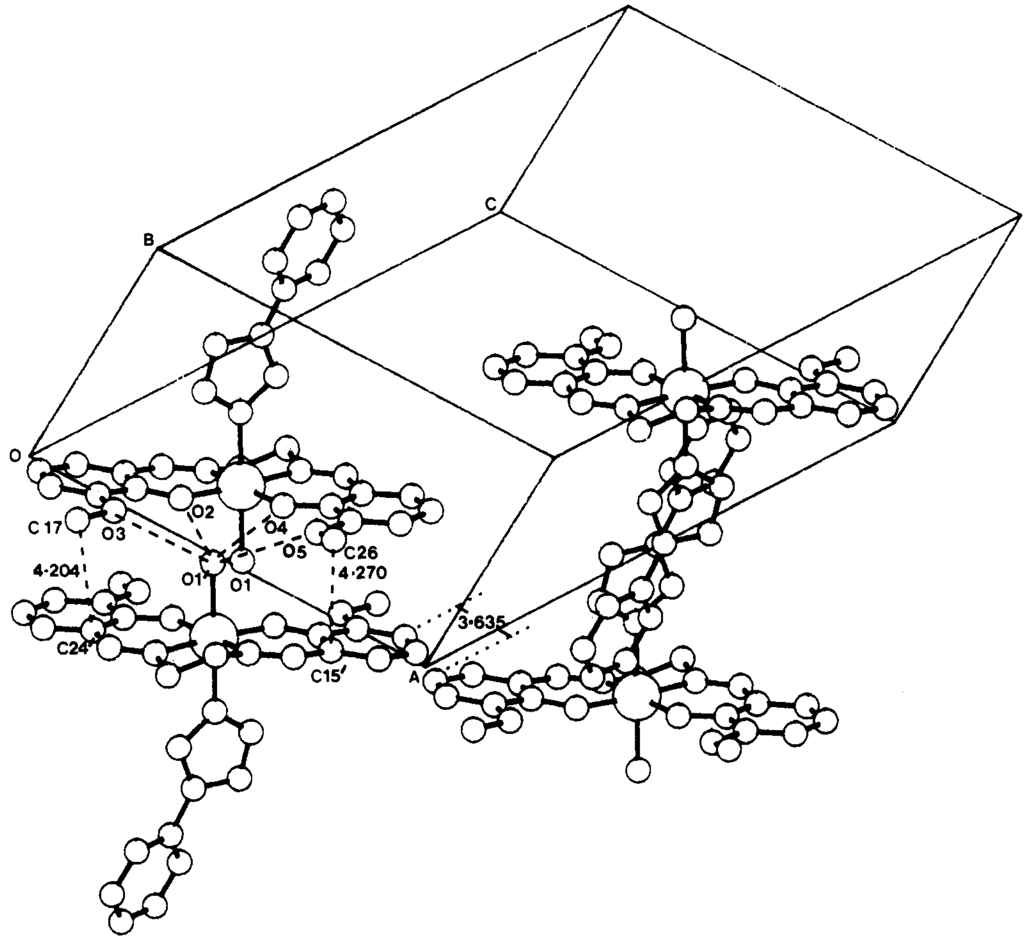

Figure 3. Lattice packing diagram showing the hydrogen-bonding interaction between iron(III) pairs. For clarity the BPh_4^- anions have been omitted. One set of hydrogen-bonding distances (Å) shown is O(1)′···O(2) = 2.858, O(1)′···O(3) = 3.108, O(1)′···O(4) = 2.89, and O(1)′···O(5) = 3.129, where the primed labels refer to the equivalent position $1 - x, \bar{y}, \bar{z}$ related by a center of symmetry to the unique asymmetric unit at x, y, z.

complexes of this type.[12,21,22] The iron atom is in the plane (within 0.07 Å) defined by the four ligand donor atoms N(3), N(4), O(2), and O(4). The whole ligand itself approximates a planar geometry that can be described by the following equation:

$$0.8769x + 0.0550y - 0.4776z = 1.592 \text{ Å}$$

The atoms C(18) and C(19) associated with the ethylenediamine link (in the gauche configuration) are at distances of 0.38 and 0.31 Å above and below the plane respectively, while all other non-hydrogen atoms are less than 0.15 Å from the plane.

The crystal lattice consists of the two ions [Fe(3-MeO-salen)(5-Ph-imd)(H_2O)]$^+$ and BPh_4^-. The closest intermolecular interactions occur between the cations that are held together in pairs by hydrogen bonding (Figure 3). The coordinated water molecule (O(1)) of the cation at the position x, y, z hydrogen bonds to the methoxy and salen donor oxygen atoms of the metal center at $1 - x, \bar{y}, \bar{z}$.

O(1) makes hydrogen bonding contacts to atoms O(2)′, O(3)′, O(4)′, and O(5)′ at the distances 2.858, 3.108, 2.887, and 3.129 Å, respectively. However, the two water molecules do not hydrogen bond with each other (i.e., O(1)...O(1)′ = 3.712 Å).

Studies of systems of this type have shown that the metal to imine nitrogen bond distance is sensitive to the spin state of the metal ion.[10,12,21,23-25] The metal–nitrogen bond distances for the high-spin complex are larger than those of the corresponding low-spin complex. In iron(III) complexes the metal to imine nitrogen distances are in the range 2.06–2.10 Å for the high-spin state and in the range 1.93–1.96 Å for the low-spin case. In the structure reported here the iron–nitrogen bonds Fe–N(3) and Fe–N(4) suggest that the metal ion is in the high-spin state, which is consistent with the ESR, magnetism, and Mössbauer results (see below).

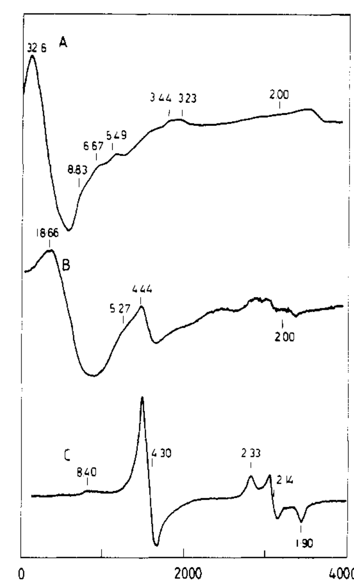

Figure 4. X-Band ESR spectra at 80 K: (A) powder sample **3**; (B) powder sample **2**; (C) sample **2** in dichloromethane (with a small amount of pyrazole added).

(21) Calligaris, M.; Nardin, G.; Randaccio, L. *Coord. Chem. Rev.* **1972**, *7*, 385.
(22) Calligaris, M.; Nardin, G.; Randaccio, L. *J. Chem. Soc., Dalton Trans.* **1974**, 1903.
(23) Hair, N. J.; Beattie, J. K. *Inorg. Chem.* **1977**, *16*, 245.
(24) Gardner, A. P.; Gatehouse, B. M.; White, J. C. B. *Acta Crystallogr., Sect. B: Struct. Crystallogr. Cryst. Chem.* **1971**, *B27*, 7505.
(25) Benson, T. H.; Bilton, M. S.; Gill, N. S. *Aust. J. Chem.* **1977**, *36*, 261.

ESR Spectra. The powder ESR spectra of all four complexes show an intense low-field line at 200–400 G (Figure 1B and 4A,B). In addition, a much weaker signal near $g = 4.3$ is observed in all cases although the relative intensities of the two lines vary from complex to complex. Some preparations also showed a number of weak lines centered near $g = 2.0$ that are probably due to small amounts of the bis adducts crystallizing out. Except for [Fe(3-EtO-salen)(5-Ph-imd)(H_2O)]BPh_4·0.5H_2O it was possible, with care, to obtain samples free of such impurities.

A line near $g = 4.3$, observed in all complexes, is generally observed in rhombically distorted high-spin Fe(III) complexes[26] and is predicted to occur as the ratio of the zero-field splitting (ZFS) parameters E/D approaches $^1/_3$, the rhombic limit. The X-ray structure of [Fe(3-MeO-salen)(5-Ph-imd)(H_2O)]BPh_4·H_2O shows that there are considerable distortions away from axial symmetry around the Fe center so the presence of such an ESR signal is not unexpected.

The origin of the low-field lines is less well established. Such signals cannot be predicted from ZFS of the $^6A_1$ ground state, for which in the rhombic limit the maximum g value is ~10 (ca. 600 G at 9.15 GHz). In addition, such lines are usually very weak. Recently, however, Hall and Hendrickson[27] have reported an ESR spectrum similar to the present for the weakly antiferromagnetically coupled[28] complex tris(pyrrolidyldithiocarbamato)iron(III) for which it was suggested that the low-field signal originated through exchange interactions.

In an attempt to better understand the solid-state ESR spectra a number of solution spectra were examined. As indicated above, the preparative solutions of [Fe(3-EtO-salen)(5-Ph-imd)(H_2O)]BPh_4·0.5H_2O show signals attributable to both high- and low-spin species at 77 K. When the pure solid complexes are dissolved in methanol, the ESR spectra just show lines near $g = 4.3$ and $g = 2$. The intensities of the low-spin lines are much weaker than those of the high spin at $g = 4.3$ (Figure 1C). Careful addition of excess Lewis base results in an increase in intensity of the low-spin lines expected for formation of the bis adduct. In methanol solutions it is likely that both coordinated molecules L and H_2O will dissociate to some extent and the equilibria discussed previously will be important.

Attempts to obtain spectra in noncoordinating solvents such as $CHCl_3$, CH_2Cl_2, or C_6H_6 were generally hindered by the limited solubility of the solid adducts in such solvents. However, CH_2Cl_2 solutions of [Fe(3-EtO-salen)(pyz)(H_2O)]BPh_4·0.5H_2O could be prepared, and these showed an intense $g \sim 4.3$ signal as well as signals at $g = 8.4$ and $g \sim 2$ (Figure 4C). In this solvent there were no signals observed in the region of 300 G in line with the hypothesis that these signals result from solid-state magnetic exchange effects (see later).

Magnetism and Mössbauer Spectra. The room-temperature magnetic moments of the mono(base) adducts fall within the range 5.8–5.9 μ_B except in the case of [Fe(3-EtO-salen)(5-Ph-imd)(H_2O)]BPh_4 (**4**), which is a little lower (Table I). As indicated previously, it was not possible to obtain samples of this derivative free of small amounts of a low-spin species that would explain the lower μ_{Fe} value.

The temperature dependence of μ_{Fe} for [Fe(3-EtO-salen)(pyz)(H_2O)]BPh_4·0.5H_2O (**2**) is shown in Figure 5 and has all the characteristics expected for a monomeric Fe(III) complex with a large zero-field splitting of the $^6A_1$ state. Further evidence on the nature of this ZFS comes from the temperature dependence of the Mössbauer spectra. A broad asymmetric quadrupole doublet is observed at 77 K that sharpens appreciably on cooling to 4.2 K (Figure 6). At the same time, the asymmetry is reduced, although surprisingly it is reversed such that the low-energy line becomes the most intense. The changes in symmetry can be explained in terms of spin relaxation.[9] For a large positive ZFS

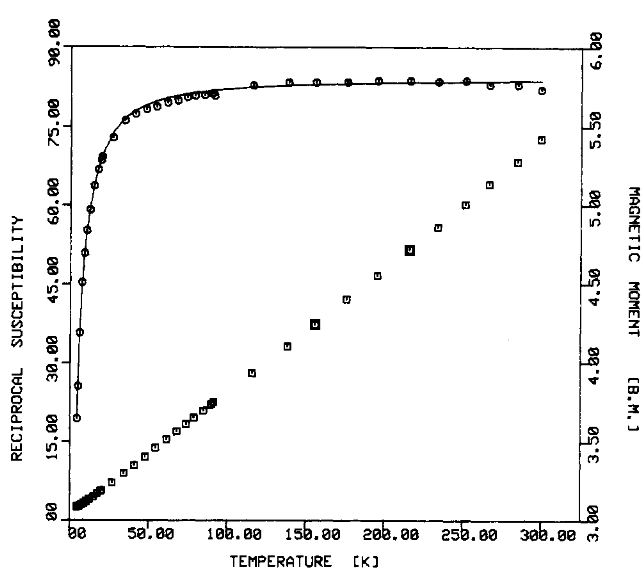

Figure 5. Magnetic moment (O) and reciprocal susceptibility (□) (per iron) vs. temperature for complex **2**. The solid line represents the best fit of the data to the parameters given in Table VI. See text for discussion.

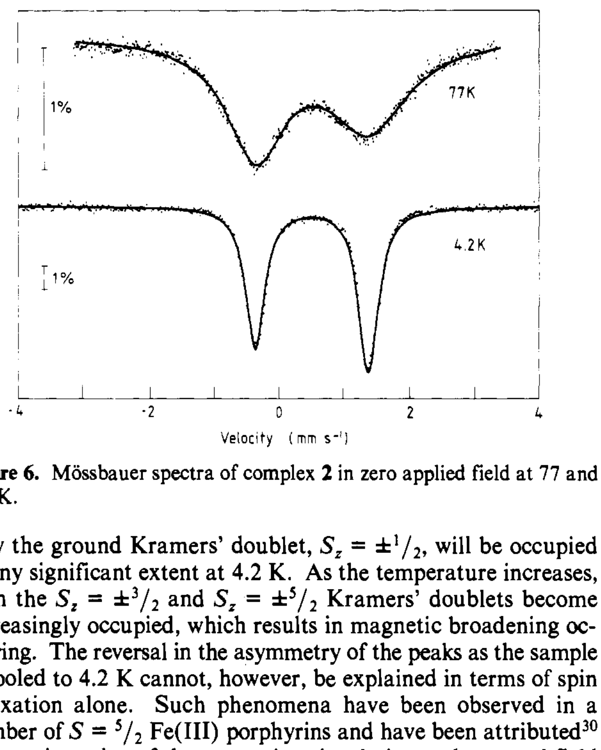

Figure 6. Mössbauer spectra of complex **2** in zero applied field at 77 and 4.2 K.

only the ground Kramers' doublet, $S_z = \pm^1/_2$, will be occupied to any significant extent at 4.2 K. As the temperature increases, both the $S_z = \pm^3/_2$ and $S_z = \pm^5/_2$ Kramers' doublets become increasingly occupied, which results in magnetic broadening occurring. The reversal in the asymmetry of the peaks as the sample is cooled to 4.2 K cannot, however, be explained in terms of spin relaxation alone. Such phenomena have been observed in a number of $S = {^5/_2}$ Fe(III) porphyrins and have been attributed[30] to a reorientation of the magnetic axis relative to the crystal field axis, although this interpretation has been questioned.[31,32] The size of the quadrupole splitting in the present complexes is notably higher than in many other high-spin Fe(III) compounds but is of similar magnitude to the values found for six-coordinate Fe(III) porphyrins.[1-4]

The observed susceptibilities were analyzed with the rhombic spin Hamiltonian

$$\mathcal{H} = g\beta\hat{H}\cdot\hat{S} + D[\hat{S}_z^2 - \tfrac{1}{3}S(S+1)] + E(\hat{S}_x^2 - \hat{S}_y^2) \quad (1)$$

and it was assumed, initially, that E/D approached the "rhombic limit" of $^1/_3$. Although it was possible to reproduce the observed

(26) Oosterhuis, W. T. *Struct. Bonding (Berlin)* **1974**, *20*, 59.
(27) Hall, G. R.; Hendrickson, D. N. *Inorg. Chem.* **1976**, *15*, 607.
(28) Cukauskas, E. J.; Deaver, B. S.; Sinn, E. *J. Chem. Soc., Chem. Commun.* **1974**, 698.
(29) Blume, M. *Phys. Rev. Lett.* **1967**, *18*, 305.
(30) Maricondi, C.; Straub, D. K.; Epstein, L. M. *J. Am. Chem. Soc.* **1972**, *94*, 4157.
(31) Gunter, M. J.; McLaughlin, G. M.; Berry, K. J.; Murray, K. S.; Irving, M.; Clark, P. E. *Inorg. Chem.* **1984**, *23*, 283.
(32) Sams, J. R.; Tsin, T. B. In "The Porphyrins"; Dolphin, D., Ed.; Academic Press: New York, 1979; Vol. IV, p 425 ff.

Table V. Mössbauer Parameters

complex	T, K	isomer shift (δ),[a,b] mm s^{-1}	quadrupole splitting (ΔE),[b] mm s^{-1}	I_1/I_2	% area
1	4.2	0.50 (1)	1.76 (1)	1.000	88.71
		0.42 (3)	0.87 (6)	1.000	11.29
	300	0.36 (2)	1.63 (2)	0.495	100
2	4.2	0.51 (1)	1.73 (1)	1.169	100
	77	0.54 (2)	1.74 (2)	0.745	100
3	4.2	0.49 (1)	1.64 (1)	1.00	96.08
		0.37 (3)	0.67 (10)	1.00	3.92
	77	0.48 (2)	1.62 (2)	1.417	100

[a] Relative to Fe metal. [b] Estimated error in last significant figure given in parentheses.

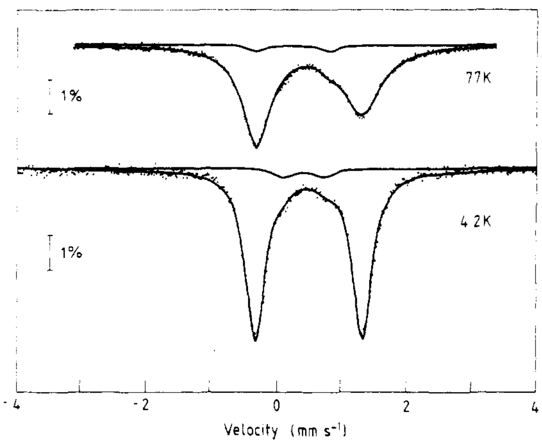

Figure 7. Mössbauer spectra of complex **3** in zero applied field at 77 and 4.2 K.

data at very low temperatures ($T < 15$ K) with unusually large ZFS parameters, $D \simeq 40$–50 cm^{-1} and $E \simeq 15$ cm^{-1}, the fit over the entire temperature range was poor. Close examination of the χ_{Fe}^{-1}/T plot showed a marked curvature at low temperatures typical of magnetic exchange, and so eq 1 was modified to consider this possibility by means of the method described recently by Berry et al.[33] Careful and systematic variation of D, E, and J showed that an acceptable fit could be obtained below ca. 100 K, although above this the observed susceptibilities were always less than those calculated. It was then decided to allow g to vary freely in the final fitting, and a good fit was obtained for the following parameter value: $D = 6.0 \pm 0.5$ cm^{-1}, $E = 0.6 \pm 0.2$ cm^{-1}, $J = -0.15 \pm 0.01$ cm^{-1}, $g = 1.97 \pm 0.02$ cm^{-1}. As seen in Figure 5 these values satisfactorily reproduce the susceptibilities over the entire temperature range. The presence of weak magnetic exchange may explain the unusual nature of the 77 K ESR spectrum that is broadened considerably (Figure 4B).

The magnetic properties of $[Fe(3\text{-MeO-salen})(pyz)(H_2O)]BPh_4$ (**1**) and $[Fe(3\text{-MeO-salen})(5\text{-Ph-imd})(H_2O)]BPh_4$ (**3**) were also studied in detail and are very similar to those just described for $[Fe(3\text{-EtO-salen})(pyz)(H_2O)]BPh_4$. However, for these two complexes the situation is complicated by the presence of small amounts of a second high-spin species, detected in the Mössbauer spectra at 4.2 K (Figure 7; Table V) and probably due to some μ-oxo dimer. The effect of such an impurity is to lower the observed susceptibilities at all temperatures, although at low temperatures the susceptibilities of μ-oxo dimers become increasingly small, so that in the region where the magnetic moments of the present complexes show their maximum temperature dependence any μ-oxo impurity present effectively acts as a diamagnetic diluent. Calculations, in which the effect of varying amounts of the μ-oxo impurity were considered, readily showed

(33) Berry, K. J.; Clark, P. E.; Murray, K. S.; Raston, C.; White, A. H. *Inorg. Chem.* **1983**, *22*, 3928.

Table VI. Best Fit Magnetic Parameters

complex	D (±0.5), cm^{-1}	E (±0.2), cm^{-1}	J (±0.01), cm^{-1}	g (±0.02)	R, %
1	4.0	1.0	−0.16	2.00	0.56
2	6.0	0.6	−0.15	1.97	0.42
3	5.0	1.5	−0.21	1.96	0.83

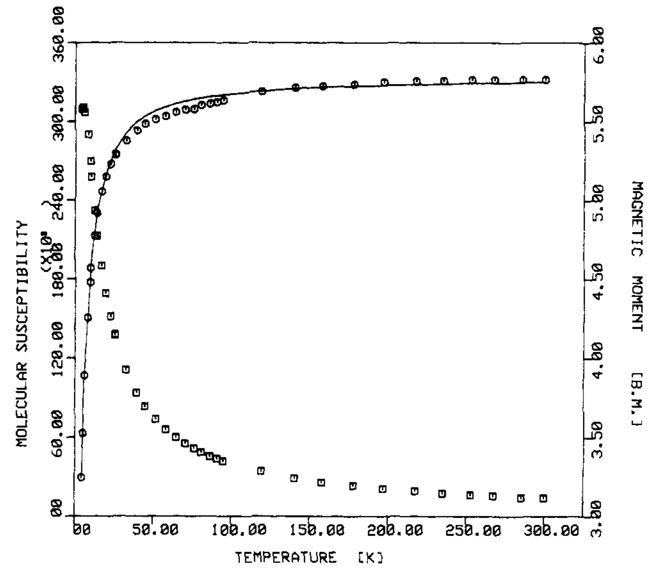

Figure 8. Magnetic moment (O) and molecular susceptibility (□) (per iron) vs. temperature for complex **3**. The solid line represents the best fit of the data to the parameters given in Table VI. See text for discussion.

the susceptibilities of these two complexes could not be explained with eq 1 alone without allowing for the presence of magnetic exchange. It was found that the influence of small amounts of μ-oxo impurities on the susceptibilities could be reproduced by allowing g to vary away from 2.0, and so in the final fitting it was chosen to vary g freely rather than correct the susceptibilities for this μ-oxo impurity. It is known that g is usually a sensitive measure of experimental uncertainties, and further it should be stressed that for $[Fe(3\text{-EtO-salen})(pyz)(H_2O)]BPh_4\cdot0.5H_2O$ there is no evidence to suggest that μ-oxo impurity is present.

Fitting of these two complexes as described above led to the best fit parameters listed in Table VI. As seen in Figure 8, there is a maximum in the susceptibility of $[Fe(3\text{-MeO-salen})(5\text{-Ph-imd})(H_2O)]BPh_4$ (**3**) at ~4.5 K, providing further support for the presence of weak exchange in these complexes. Measurements at temperatures less than 4.2 K would be needed to observe similar maxima for the two pyrazole adducts studied.

The weak antiferromagnetic exchange observed in **3** presumably originates through the pairwise interactions described above and shown in Figure 3. If a superexchange pathway via H-bonded fragments of the type Fe–OH_2–O(salen)–Fe is involved, then J would be expected to be very small, as is observed. It is always difficult to unambiguously apportion superexchange and direct metal–metal (e.g., dipole–dipole) contributions to the overall exchange coupling. Interestingly, the high-spin Co(II) complex $Co(3\text{-MeO-salen})(H_2O)$ shows the same kind of H-bonded dimeric structure[34] as is observed here, and a weak antiferromagnetic exchange contribution was also required to explain its low-temperature magnetization data.[35]

Relations to Aquoiron(III) Heme Proteins. The two different axial ligands in complexes such as **3** are similar to those found in aquometheme proteins, and it is pertinent to briefly compare the structural and electronic features. The iron–water Fe–O bond length of 2.205 Å is somewhat longer than the range of values (1.98–2.10 Å) normally found in Fe^{III}–OH_2 bonded complexes,[23]

(34) Calligaris, M.; Nardin, G.; Randaccio, L. *J. Chem. Soc., Dalton Trans.* **1974**, 1903.
(35) Kennedy, B. J.; Murray, K. S., unpublished data.

including for instance $[Fe(TPP)(H_2O)_2]^+$, which has a distance of 2.09 Å.[1] It is also longer than the 2.0-Å value assumed in sperm whale aquometmyoglobin.[15] The Fe–N(imidazole) distance of 2.132 Å is, however, similar to the corresponding distance in aquometmyoglobin and in horse hemoglobin.[15] An out-of-plane displacement of Fe of some 0.4 Å has been reported for the myoglobin structure whereas the present "in-plane" structure would support the reservations expressed by Scheidt and Reed[1] concerning the probable overestimation of such a displacement.

The high-spin ground state for the present complexes generally mirrors that of the aquomethemes although the zero-field splittings are less than those deduced for $MetHb(H_2O)$ from Mössbauer,[36] ESR,[37] and susceptibility measurements,[38] viz. $D \sim 10\ cm^{-1}$. Such differences in detail are perhaps not surprising in view of the relative ligand field symmetries and strengths of the Schiff-base and porphyrin systems. The similarity of the quadrupole splittings in the Mössbauer spectra of the protein and of the present compounds suggests, nevertheless, a not too dissimilar overall ligand field environment around the Fe atom.

Acknowledgment. This work was supported by grants from the Australian Research Grants Scheme and the Monash University Special Research Grants Fund. The authors are grateful to Dr. J. D. Cashion and students in the Physics Department at Monash University for generous help with Mössbauer measurements.

Registry No. 1, 95674-15-0; 2, 95674-17-2; 3, 95674-20-7; 4, 95674-22-9; Fe(3-MeO-salen)Cl, 62945-14-6; Fe(3-EtO-salen)Cl, 95674-23-0.

Supplementary Material Available: Listings of atom coordinates, anisotropic thermal parameters, and observed and calculated structure factors (20 pages). Ordering information is given on any current masthead page.

(36) Lang, G.; Asakura, T.; Yonetani, T. *Biochim. Biophys. Acta* **1970**, *214*, 381.
(37) Eisenberger, P.; Pershan, P. S. *J. Chem. Phys.* **1967**, *47*, 3327.
(38) Tasaki, A.; Otsuka, J.; Kotani, M. *Biochim. Biophys. Acta* **1967**, *140*, 284.

Contribution from the Departments of Chemistry, University of Vermont, Burlington, Vermont 05405, and University of Arkansas, Fayetteville, Arkansas 72701

Organophosphazenes. 18. Friedel–Crafts Phenylation Reactions of Alkyl- and (Dimethylamino)fluorocyclotriphosphazenes[1]

CHRISTOPHER W. ALLEN,*[2a] SCOTT BEDELL,[2a] WILLIAM T. PENNINGTON,[2b] and A. WALLACE CORDES[2b]

Received August 8, 1984

The (dimethylamino)- and butylpentafluorocyclotriphosphazenes, $N_3P_3F_5R$ ($R = N(CH_3)_2$, n-C_4H_9, t-C_4H_9), undergo the Friedel–Crafts phenylation reaction to yield $N_3P_3F_4(C_6H_5)R$. A geminal configuration was assigned to each of the phenyl derivatives on the basis of the NMR (^1H, ^{13}C, ^{31}P) spectroscopic data. The crystal and molecular structures of $N_3P_3F_4(C_6H_5)(t\text{-}C_4H_9)$ have been determined; the crystals are orthorhombic, space group *Pmma*, with $a = 7.264$ (1) Å, $b = 12.204$ (2) Å, $c = 17.028$ (3) Å, $V = 1509.5$ (7) Å^3, and $Z = 4$. The final refinement gave $R = 0.042$ and $R_w = 0.054$ for 1087 observed reflections. The molecule, which has a crystallographically imposed mirror plane of symmetry, has the predicted geminal arrangement of organic groups and P–N distances of 1.618 (1), 1.527 (2), and 1.565 (1) Å. The central P–N ring is planar within 0.007 Å. Bond angles are as follows: C–P–C = 108.9 (1)°; F–P–F = 96.36 (9)°; N–P–N = 114.1 (1), 120.91 (9)°; P–N–P = 122.58 (9), 118.9 (1)°. The observation of Friedel–Crafts phenylation of the alkylphosphazenes demonstrates that π donation from an exocyclic substituent is not a necessary prerequisite for this reaction.

Introduction

Friedel–Crafts arylation is a classic reaction[3] in phosphazene chemistry dating back to the pioneering studies of Bode and Bach.[4] The reaction can be used to produce geminal aryl groups in chloro[4,5] and fluorocyclophosphazenes.[6] The observation that the reaction usually yields geminal di-, tetra-, and hexaarylphosphazenes but not mono-, tri-, or pentasubstituted derivatives leads to the suggestion that a ≡PPhCl center is more reactive than a $\equiv PCl_2$ center. Aminochlorophosphazenes also undergo the Friedel–Crafts arylation reaction, which allows for conversion of a $\equiv PClNR_2$ center to a $\equiv P(Ph)NR_2$ center.[7] Depending on the nature of the amine, side reactions may also become significant. The phosphazo substituent also promotes Friedel–Crafts arylation at a $\equiv PCl(N{=}PPh_3)$ center.[8]

In spite of the synthetic utility of this reaction, little is known about the mechanism. The first step of the reaction is often assumed to be the formation of a phosphonium ion arising from halide abstraction by the Lewis acid:

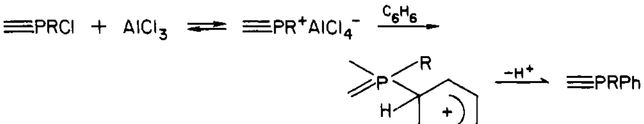

Definitive evidence on this point has yet to become available. The addition compounds of aluminum tribromide with halocyclotriphosphazenes, $N_3P_3X_6{\cdot}nAlBr_3$ ($X = Cl$, $n = 1$; $X = Br$, $n = 1, 2$) are believed to have the aluminum tribromide entity coor-

(1) Part 17: Allen, C. W.; Descorcie, J. L.; Rmachandran, K. *J. Chem. Soc., Dalton Trans.* **1984**, 2843.
(2) (a) University of Vermont. (b) University of Arkansas.
(3) Allcock, H. R. "Phosphorus-Nitrogen Compounds"; Academic Press: New York, 1972. Krisnamurthy, S. S.; Sau, A. C.; Woods, M. *Adv. Inorg. Chem. Radiochem.* **1978**, *21*, 41.
(4) Bode, H.; Bach, H. *Chem. Ber.* **1942**, *75*, 215.
(5) Acock, K. G.; Shaw, R. A.; Wells, F. B. G. *J. Chem. Soc.* **1964**, 121. Grushkin, B.; Sanchez, M. G.; Ernest, M. V.; McClanahan, J. L.; Ashby, G. E.; Rice, R. G. *Inorg. Chem.* **1965**, *4*, 1538. McBee, E. T.; Okuhara, K.; Morton, C. J. *Inorg. Chem.* **1965**, *4*, 1672.
(6) Allen, C. W.; Tsang, F. Y.; Moeller, T. *Inorg. Chem.* **1968**, *7*, 2183. Allen, C. W.; Moeller, T. *Inorg. Synth.* **1970**, *12*, 293. Allen, C. W.; Brunst, G. E.; Perlman, M. E. *Inorg. Chim. Acta* **1980**, *41*, 265. Allen, C. W.; Toch, P. L. *Inorg. Chem.* **1981**, *20*, 8.
(7) Das, S.; Shaw, R. A.; Smith, B. C. *Angew. Chem., Int. Ed. Engl.* **1968**, *7*, 887. Das, S.; Shaw, R. A.; Smith, B. C. *J. Chem. Soc., Dalton Trans.* **1981**, 107. Das, S.; Hasan, M. U.; Shaw, R. A.; Smith, B. C.; Woods, M. *Z. Naturforsch., B: Anorg. Chem., Org. Chem.* **1979**, *34B*, 58.
(8) Biddlestone, M.; Shaw, R. A. *J. Chem. Soc., Dalton Trans.* **1973**, 2740.

0020-1669/85/1324-1653$01.50/0